An Improved Driving Method for Synchronous Rectifier Using Drain-Source Voltage Sensing

Dong Wang
Member, IEEE
dong.wang@queensu.ca

Liang Jia
Student Member, IEEE
liang.jia@queensu.ca

Yan-Fei Liu
Senior Member, IEEE
yanfei.liu@queensu.ca

Paresh C Sen
Life Fellow, IEEE
senp@queensu.ca

Department of Electrical and Computer Engineering, Queen's University
Kingston, Ontario, Canada. K7L 3N6

***Abstract*— Traditional voltage sensing method has already been widely used for the synchronous rectifier. However, the parasitic parameters will cause the false turn-on and early turn-off problem. In this paper, the conception of zero-crossing noise filter is presented. By applying this filter to the synchronous rectifier, the false turn-on and early turn-off problem can be resolved. Only three passive components are needed in the proposed filter which makes it reliable and easy to implement. Simulation and experimental results show that the zero-crossing noise filter can significantly improve the reliability as well as the efficiency of the power circuit. A 400V to 12V 100W Flyback converter and a 600W half bridge LLC resonant converter prototype are built to verify the advantages of the new zero-crossing noise filter.**

I. INTRODUCTION

With the ever-increasing demands for telecommunication and computer system, the needs for power supplies with low voltage high current output keeps increasing. In order to reduce the loss caused by the high output current, synchronous rectifier (SR) is usually used to replace output Schottky barrier diodes[1, 2]. However, due to the existence of the parasitic parameters, as well as the load condition, the time of the switch on and off of the SR are not always synchronous with the primary MOSFET. In these circumstances, if the SR is driven by an incorrect gate signal, it will cause unnecessary power loss, even the damage of the system.

To generate accurate driving signal for the SR, many studies have been done in recent years. All of these schemes can be divided into self-driven and external-driven. Self-driven method uses the voltage of some deliberate points where the waveforms are similar to the driving signal of the SR[3-8]. It's obvious that this driving method can only be applied to the specific topologies such as those with LC output filters.

External-driven method can also be sorted as current sensing type and voltage sensing type. Current sensing method detects the current through the SR to generate the gate drive signal[9]. A bulky current-sensing transformer (CT) is needed for this method and the extra conduction loss of the winding and the solder joints will be caused. Undesired delay at turn-on of the SR is also inevitable because of the turn-on threshold that will cause duty cycle loss of the SR. Some literatures have figured out how to use the auxiliary winding or primary CT as the substitutes to the CT of the SR to reduce the size and conduction loss[10-12]. However, the increasing of the volume and the weight as well as the loss of the converter are inevitable due to the extra winding.

Voltage sensing method uses the R_{ds_on} of the SR as a current shunt and detects the voltage across the drain to the source (v_{DS}) of the SR to generate the driving signal[13-15]. Many driving chips have been developed based on this method to simplify the SR driving. However, the sensed v_{DS} of the MOSFET is actually the sum of the R_{ds_on} voltage drop and the package's inductive voltage drop. A nano Henry (nH) inductance introduced by PCB trace will cause a considerable duty cycle loss. Therefore, the SR will be on for a much shorter time than required, resulting in extra conduction loss[16]. Moreover, due to the small R_{ds_on} of the MOSFET, the voltage rating of the detecting threshold is only several millivolts. Thus even a very small zero-crossed ringing caused by the parasitic parameters of the circuit may result in the false gate driving signal. All the existing driving chips use a minimum conduction time (MCT) to blank the parasitic ringing. If not used properly, this approach will cause circulating current or damage of the power circuit at certain load condition.

In this paper, a new driving method for the SR based on the v_{DS} sensing scheme is presented. By applying a zero-crossing noise filter between the drain and the source of the SR, the false triggering can be effectively eliminated. The resistor and the capacitor in the filter are also used to compensate the duty cycle loss caused by the trace inductance of the MOSFET package. There are only three passive components in this filter, making the driving scheme reliable and easy to be implemented. A 400V to 12V 100W Flyback and a 600W half bridge LLC resonant converter prototype are built to validate the theoretical analysis.

978-1-4244-8083-8/11/$26.00 ©2011 IEEE

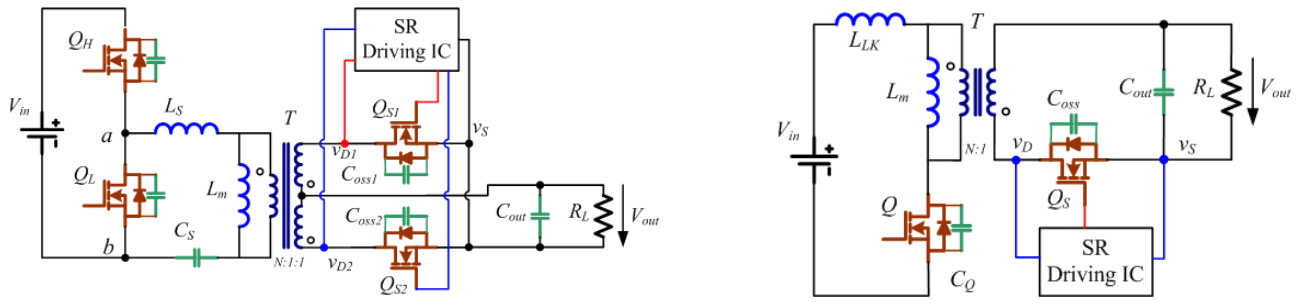

(a) LLC converter (b) Flyback Converter

Fig. 1. Typical applications of SRs

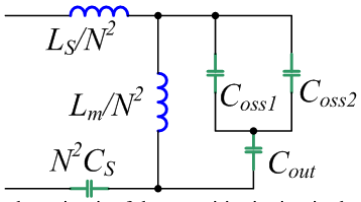

Fig. 2. Equivalent circuit of the parasitic ringing in the LLC resonant converter

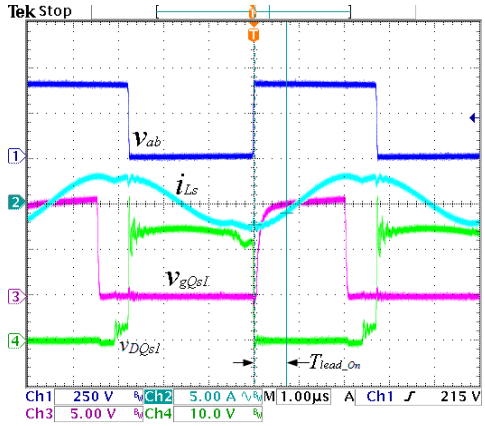

Fig. 3. False-turn-on of SR under light load condition in the resonant LLC converter

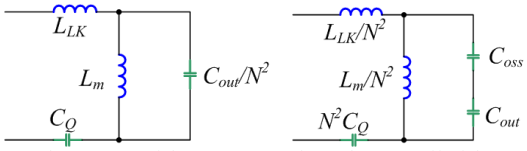

(a) at the turn-on of the SR (b) at the turn-off of the SR

Fig. 4. Equivalent circuits of the parasitic ringings in the Flyback converter

II. Problems of The Traditional Voltage Sensing SRs Driving Method

In order to illustrate the problems of the traditional voltage sensing SR driving method, half-bridge LLC resonant converter and flyback converter with SRs are selected as the examples. Fig. 1 shows the circuit diagrams of the typical half-bridge LLC resonant converter and the flyback converter with SRs. The problems of traditional voltage sensing method can be listed as false turn-on and early turn-off problems.

A. False-triggering problems of the SRs

1) False-turn-on problem of the LLC resonant converter

Due to the leakage inductance and output capacitance of the SR FET, the voltage across the SR rings before and after the SR conducts. The equivalent circuit of the parasitic ringing is shown in Fig. 2. When the SRs turn off, L_S resonate with the output capacitance (C_{oss}) of the SRs. If the voltage spikes reach the SR turn on threshold, especially at light load condition, the SR will be false-triggered. This will result in the energy reverse from the output capacitor to the input source or even breakdown of the power circuit during the transient time. Fig. 3 shows the false-turn-on of the SR at light load condition.

The frequency of the parasitic ringing can be calculated from Fig. 2. To simplify the analysis, assume that

$$C_{oss1} = C_{oss2} = C_{oss} \tag{1}$$

Comparing the leakage inductance of the transformer with the output capacitance of the SRs, the influences of the magnetizing inductance L_m, the series resonant capacitor C_S and the output capacitor C_{out} can be neglected. The ringing frequency can be derived as

$$f_{ringing} = \frac{1}{2\pi \cdot \sqrt{\frac{L_S}{N^2} \cdot 2C_{oss}}} \tag{2}$$

2) False-turn-on problem of the Flyback converter

When the primary MOSFET of the Flyback converter turns off, the energy stored in the magnetizing inductor L_m begins to release to the load and the SR is turned on. At the same time, the leakage inductance L_{LK} begins to resonate with the parallel capacitor C_Q, as shown in Fig. 4 (a). The ringing frequency can be derived

$$f_{riinging\_on} \approx \frac{1}{2\pi \cdot \sqrt{L_{LK} \cdot C_Q}} \tag{3}$$

Fig. 5 shows the turn-on parasitic ringing of v_{ds_Qs}. This ringing will inevitably result in the SR false turn-off if it is

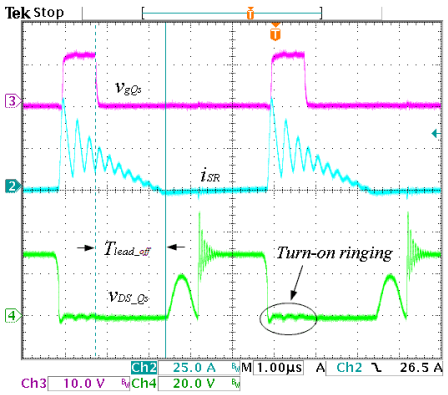

Fig. 5. Parasitic ringing at the turn-on of the SR in the Flyback converter

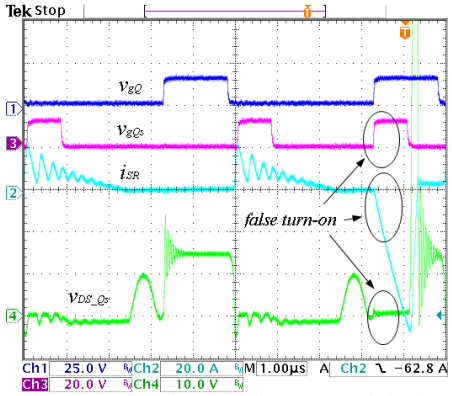

Fig. 6. False-turn-on of the SR under DCM mode in the Flyback converter

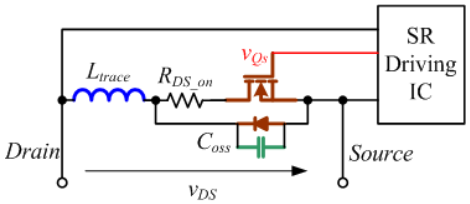

Fig. 7. v_{DS} sensing method for the SR

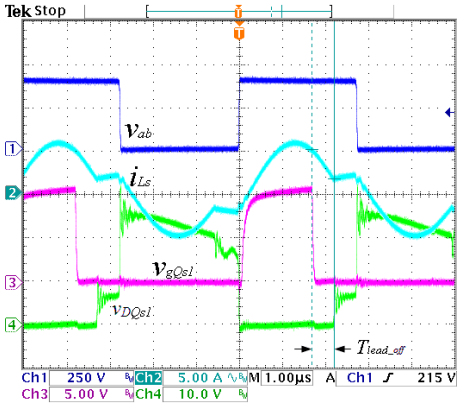

Fig. 8. Lead-turn-off of the SR in LLC converter

not blanked. All of the commercial driver chips for the SR adopt a minimum conduction time (MCT) to blank the ringing at the turn-on of SR. If not used properly, this blanking method will causes the damage of the converter as explained following.

The parasitic ringing also exists at the turn-off of the SR when the Flyback converter operates under DCM mode. When the energy stored in the magnetizing inductor L_m is totally released to the load, L_m begins to resonate with the parallel capacitor C_Q of the primary MOSFET[1]. The equivalent circuit of the parasitic ringing at turn-off of the SR can be deduced from Fig. 1 (b), as shown in Fig. 4 (b). If the ringing causes the voltage across the SR reaching its turn on threshold, the SR will be false-triggered, and stay at ON state due to the existence of the MCT of the driver chip, even if the polarity of the voltage across the SR changed. If the primary MOSFET is turned on during the SR ON time, the currents through the primary MOSFET and the SR increase rapidly, and then damage the circuit. The false turn-on of the SR in the Flyback converter is shown in Fig. 6. The ringing frequency can be derived as

$$f_{ringing\_off} \approx \frac{1}{2\pi \cdot \sqrt{(L_{LK} + L_m) \cdot C_Q}} \tag{4}$$

B. *Duty cycle loss problems of the SRs*

The equivalent circuit of the SR with driving circuit is shown in Fig. 7. When the SR is turned on, the body diode is bypassed. Compared with the R_{DS_on}, the impedance of the C_{oss} is much larger and can be neglected. Because of the trace inductance, the voltage v_{DS} leads the current i_{SR}. As for the LLC resonant converter, the current through the SR can be approximated as the half period of the sinusoidal waveform. Therefore, the lead time of the v_{DS} to the i_{SR} can be derived as

$$\theta_{lead} = \tan^{-1}\left(\frac{\omega_0 \cdot L_{trace}}{R_{DS\_on}}\right) \tag{5}$$

$$T_{lead} = \frac{\theta_{lead}}{\omega_0} \tag{6}$$

where ω_0 is the series resonant frequency of the resonant tank. As for the flyback converter, because the magnetizing inductance of the transformer is far more than the lead inductance of the SR, the decreasing rate of the current through the SR is dominated by the magnetizing inductances and the output voltage. Therefore, the lead time of the v_{DS} to the i_{SR} can be derived as

$$T_{lead} = \frac{L_{trace}}{R_{DS\_on}} \tag{7}$$

It is observed that if the v_{DS} is detected directly to generate the driving signal of the SR, the duty cycle loss is inevitable. Fig. 8 shows the lead-turn-off of the SR in the LLC resonant converter when v_{DS} of the SR is fed to the driving IC. The same result in the flyback converter can also be observed in Fig. 5 and Fig. 6

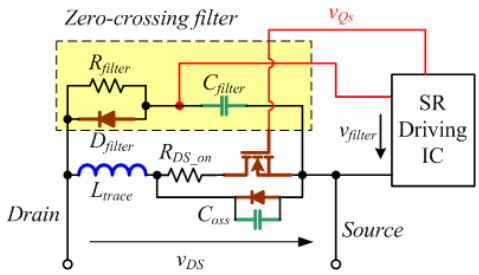

Fig. 9.Equivalent circuit of the SR with the zero-crossing noise filter

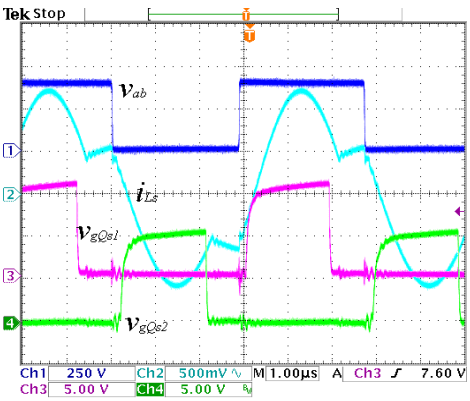

Fig. 11. Experimental waveforms of the LLC converter with zero-crossing filter at full load condition

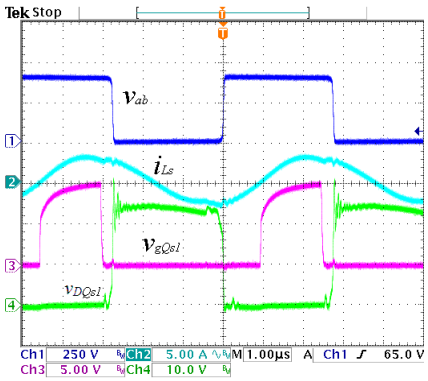

Fig. 12. Experimental waveforms of the LLC converter with zero-crossing filter at light load condition

TAB. 1. PARAMETERS OF THE PROTOTYPE

LLC converter		*Flyback converter*	
L_m (µH)	98.7	L_m (µH)	98.7
L_S , L_{LK}(µH)	9.8	L_{LK} (µH)	9.8
C_S (nF)	40		
Turns ratio	20:1:1	Turns ratio	20: 1
Q_H, Q_L	STP26NM60N	Q	STB11NM80
Q_{S1}, Q_{S2}	SIR158DP	Q_S	SIR158DP
zero-crossing filter			
R_{filter} (kΩ)	3.9	C_{filter} (pF)	100
D_{filter}	1N4148		

III. NEW DRIVING METHOD FOR SR WITH ZERO-CROSSING FILTER

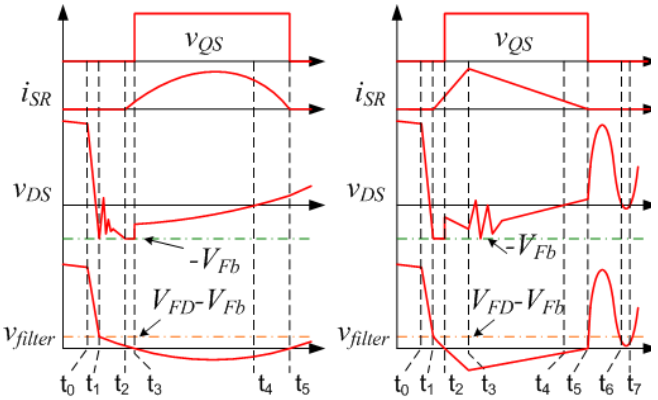

(a) for LLC converter (b) for Flyback converter

Fig. 10. Key waveforms of the SR with the zero-crossing noise filter

To solve the false turn-on problem, a zero-crossing filter can be added to filter out the high frequency parasitic ringing. The equivalent circuit of the SR with zero-crossing noise filter is shown in Fig. 9 in which the forward voltage of the D_{filter} (V_{FD}) should be a little larger than that of the body diode of the SR (V_{Fb}). Two diodes need to be connected in series if this condition can't be met by one diode. In the diagram, v_{filter} is sensed by the SR driving IC as the substitutes of v_{DS}. The key waveforms of the SR with zero-crossing filter applied for LLC and Flyback converter are illustrated in Fig. 10. At the turn-on of the SR, due to the existence of the zero-crossing filter, the high frequency parasitic ringing is blanked. At the turn-off of the SR in the Flyback converter, the frequency of parasitic ringing is very low. But the time interval that v_{DS} across the turn-on threshold is very short. Therefore, the zero-crossing filter can also filter it out.

To compensate the lead time at the switch off of the SR, the parameters of the zero-crossing noise filter should be selected carefully to match the trace inductance and R_{DS_on} of the SR. The parameters of the filter are chosen specifically to emulate the lead angle θ_{lead} so that the voltage across the C_{filter} can describe v_{RDS_on} exactly. The parameters of the filter is defined as

$$R_{filter}C_{filter} = \frac{L_{trace}}{R_{DS\_on}} \tag{8}$$

There are two premises for the zero-crossing filter to emulate the current through the SR. One is that the parameters of the R_{filter} and C_{filter} should be matched to the trace inductance and R_{DS_on} of the SR, as shown in equation (8). The other is that the initial condition of the voltage v_{filter} is zero. Due to the deliberately designed parameters of the R_{filter} and C_{filter} as well as the small value between V_{FD}-V_{Fb} and the turn on threshold, both of these two premises can be met. In addition, the false-triggering immunity of the zero-crossing noise filter is still retained. Consequently, the reliability of the circuit is improved and the conduction loss is significantly reduced.

IV. EXPERIMENTAL RESULTS

To verify the theoretical analysis in the previous section, a 400V to 12V 100W Flyback and a 600W half-bridge LLC resonant converter prototype are built. The parameters of the circuit are listed in Tab. 1.

Fig. 11 and Fig. 12 illustrate the experimental waveforms of the LLC converter with SR and zero-crossing noise filter at full load and light load conditions. It shows that the SR with zero-crossing noise filter can operate properly at any load condition.

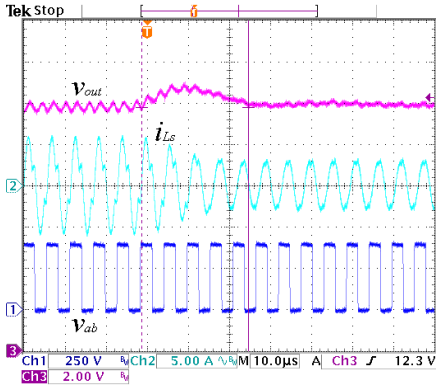

Fig. 13. Load transient test from full load to light load condition of the LLC converter

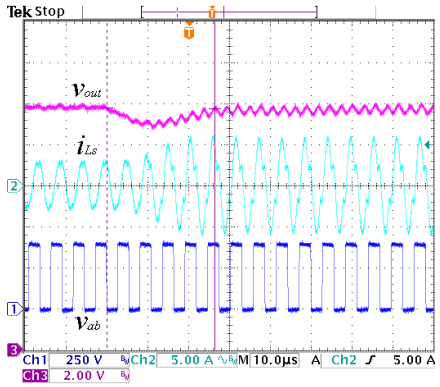

Fig. 15. Load transient test from light load to full load condition of the LLC converter

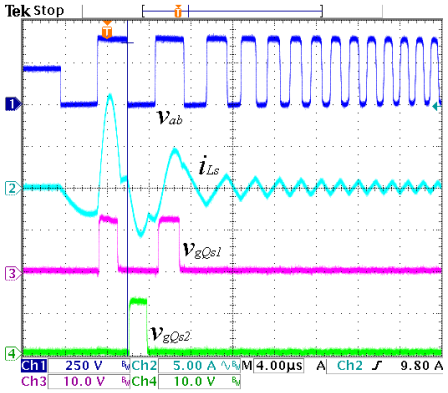

Fig. 17. Burst mode test of the LLC converter with zero-crossing noise filter

Fig. 13 ~ Fig. 17 show the transient tests of the LLC converter with zero-crossing filter. Fig. 13 and Fig. 14 shows the experiment results from full load (50A) to light load (5A) condition. Fig. 15 and Fig. 16 show the results from light load (5A) to full load (50A) condition. Fig. 17 shows the converter operates under burst mode condition (0.5A). The experiment results demonstrate that the zero-crossing noise can operate under transient condition properly.

Fig. 18 and Fig. 19 show the experimental waveforms of a flyback converter with SR and zero-crossing filter. It

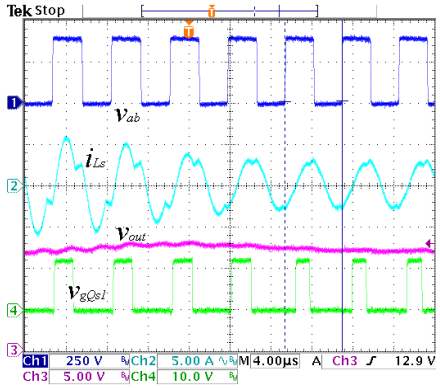

Fig. 14. Detail waveforms of the transient test from full load to light load condition

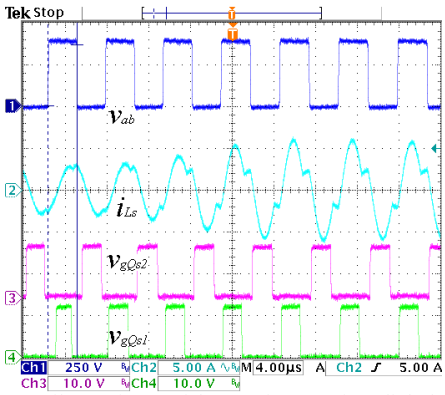

Fig. 16. Detail waveforms of the transient test from light load to full load condition

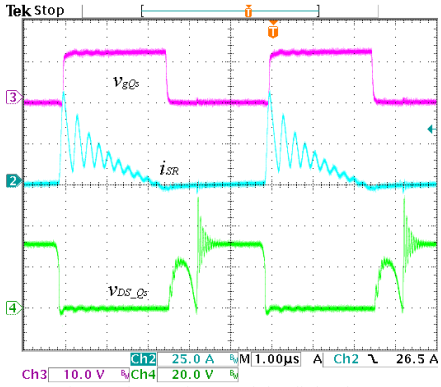

Fig. 18. Experimental waveforms of the flyback converter with SR and zero-crossing filter in DCM mode

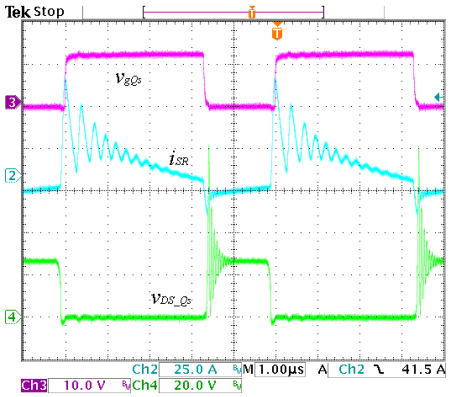

Fig. 19. Experimental waveforms of the flyback converter with SR and zero-crossing filter in CCM mode

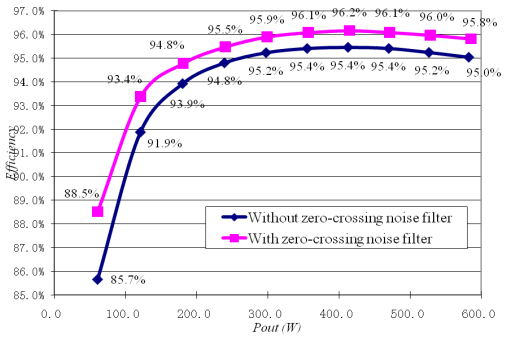

Fig. 20. Efficiency comparison of the LLC converter with and without the zero-crossing noise filter

is observable that the parasitic ringing at both the turn-on and the turn-off are filtered out. The duty cycle loss at the turn-off of the SR is also compensated. Moreover, the zero-crossing filter can also operate at CCM mode.

Fig. 20 compared the measured efficiency of the LLC converter prototype between with and without zero-crossing noise filter at different load condition. It shows clearly that whatever the load condition is, the proposed driving method can effectively improve the efficiency of the circuit.

V. CONCLUSION

Due to the easy implementation and small profile, the traditional voltage sensing method has already been widely used for the synchronous rectifier. However, the parasitic parameters in the circuit will cause the false turn-on and lead turn-off problem which undermine the reliability of the converter. In this paper, the conception of zero-crossing noise filter is presented. By applying this filter to the MOSFET, the false turn-on and lead turn-off problem can be resolved. Only three passive components are needed in the proposed filter which makes it reliable and easy to implement. Simulation and experimental results show that the zero-crossing noise filter can significantly improve the reliability as well as the efficiency of the power circuit. Half-bridge LLC resonant converter and Flyback converter with SRs are selected as the examples to prove that this zero-crossing noise filter can also be applied to any other SR circuit. A 400V to 12V 100 W Flyback and a 600W half bridge LLC resonant converter prototype are built to verify the theoretical analyses.

REFERENCES

[1] M. T. Zhang, M. M. Jovanovic, and F. C. Y. Lee, "Design considerations and performance evaluations of synchronous rectification in flyback converters," *IEEE Trans. Power Electron.*, vol. 13, no. 3, pp. 538-546, 1998.

[2] D. Z. Jiao, J. M. Zhang, X. G. Xie, et al., "A novel current driven synchronous rectifier," in *Proc. Int. Power Electron. Drive Syst. Conf.*, 2003, pp. 343-346 Vol.1.

[3] Y. Gu, Z. Lu, Z. Qian, et al., "A novel driving scheme for synchronous rectifier suitable for modules in parallel," *IEEE Trans. Power Electron.*, vol. 20, no. 6, pp. 1287-1293, 2005.

[4] M. Xu, Y. Ren, J. Zhou, et al., "1-MHz self-driven ZVS full-bridge converter for 48-V power pod and DC/DC brick," *IEEE Trans. Power Electron.*, vol. 20, no. 5, pp. 997-1006, 2005.

[5] P. Alou, J. A. Cobos, O. Garcia, et al., "A new driving scheme for synchronous rectifiers: single winding self-driven synchronous rectification," *IEEE Trans. Power Electron.*, vol. 16, no. 6, pp. 803-811, 2001.

[6] Y. Sung-Pei, L. Jong-Lick, and C. Shin-Ju, "A novel ZCZVT forward converter with synchronous rectification," *IEEE Trans. Power Electron.*, vol. 21, no. 4, pp. 912-922, 2006.

[7] A. Fernandez, J. Sebastian, M. M. Hernando, et al., "New self-driven synchronous rectification system for converters with a symmetrically driven transformer," *IEEE Trans. Ind. Appl.*, vol. 41, no. 5, pp. 1307-1315, 2005.

[8] A. Fernandez, D. G. Lamar, M. Rodriguez, et al., "Self-Driven Synchronous Rectification System With Input Voltage Tracking for Converters With a Symmetrically Driven Transformer," *IEEE Trans. Ind. Electron.*, vol. 56, no. 5, pp. 1440-1445, 2009.

[9] X. Xie, J. C. P. Liu, F. N. K. Poon, et al., "A novel high frequency current-driven synchronous rectifier applicable to most switching topologies," *IEEE Trans. Power Electron.*, vol. 16, no. 5, pp. 635-648, 2001.

[10] X. Wu, G. Hua, J. Zhang, et al., "A New Current Driven Synchronous Rectifier for Series-Parallel Resonant (LLC) DC-DC Converter," *IEEE Trans. Ind. Electron.*, vol. PP, no. 99, pp. 1-1, 2010.

[11] B. Yuan, M. Xu, X. Yang, et al., "A new structure of LLC with primary current driven synchronous rectifier," in *Proc. IEEE Power Electron. Motion Control Conf.*, 2009, pp. 1266-1269.

[12] X. Wu, B. Li, Z. Qian, et al., "Current driven synchronous rectifier with primary current sensing for LLC converter," in *Proc. IEEE Energy Conv. Cong. Expos.*, 2009, pp. 738-743.

[13] B.-S. Kim, H.-S. Ryu, M.-S. Shin, et al., "Design of Flyback Converter with Voltage Driven Synchronous Rectifier," in *Proc. EPE Power Electron. Motion Control Conf.*, 2006, pp. 631-635.

[14] H. Pan, Y. C. Liang, and R. Oruganti, "Design of smart power synchronous rectifier," *IEEE Trans. Power Electron.*, vol. 14, no. 2, pp. 308-315, 1999.

[15] X. Zhou, M. Donati, L. Amoroso, et al., "Improved light-load efficiency for synchronous rectifier voltage regulator module," *IEEE Trans. Power Electron.*, vol. 15, no. 5, pp. 826-834, 2000.

[16] D. Fu, Y. Liu, F. C. Lee, et al., "A Novel Driving Scheme for Synchronous Rectifiers in LLC Resonant Converters," *IEEE Trans. Power Electron.*, vol. 24, no. 5, pp. 1321-1329, 2009.